Diffusion on a stepped substrate: Collective diffusion in the Langmuir gas model

J. Merikoski* and S. C. Ying
Department of Physics, Brown University, Box 1843, Providence, Rhode Island 02912
(Received 7 February 1997)

We study collective diffusion of adatoms on a stepped substrate within a Langmuir gas model. Our model allows for modified potential barriers and wells near the step edges, as well as different prefactors for intrinsic jump rates at step edges. The diffusion tensor is calculated using projection operator techniques. We study in detail the dependence of the macroscopic collective diffusion on the microscopic parameters in the model. Collective effects due to finite coverage turn out to be crucial in determining the influence of steps on measurable activation barriers and effective prefactors already at low coverage. [S0163-1829(97)03928-3]

I. INTRODUCTION

In the study of surface dynamics, many important processes such as thin film growth and spreading of density profiles depend crucially on the macroscopic collective diffusion rate.[1] Since this rate is concerned with the motion of the adsorbate over macroscopic distances, it is unavoidably affected by the existence of surface defects, especially in the form of impurities and surface steps[2] even on a well-prepared sample substrate. Scanning tunneling microscope (STM) and field emission studies have confirmed the prediction[3] that there exist extra activation barriers at the steps leading to a different microscopic mobility for adsorbates there as compared to the flat terrace region. The collective diffusion rate has been studied experimentally by various methods.[4–7] However, there exist only limited efforts[7,8] in trying to understand how macroscopic collective diffusion depends on the microscopic jump rates near the steps. This is the question we address in this paper.

In an earlier study, diffusion of a single atom on a stepped substrate with a periodic array of straight steps was studied within a lattice-gas model by Natori and Godby.[9] In this work, we generalize this model to study collective diffusion at finite coverages within a Langmuir gas model, where the ''interaction'' between adsorbate particles is the exclusion of double occupancy in lattice sites. The model includes the effect of the Schwoebel barrier, extra binding at step edge, and the enhanced diffusion along step edges. We solve the model using a variety of approaches including the Mori projection operator formalism,[10] Green's functions techniques,[11,12] and Monte Carlo (MC) simulations.[13] In the presence of the extra binding at step edges, the collective effects turn out to totally change the physics already at relatively low coverage. A preliminary report of some of the results presented in this paper has already been given in Ref. 14, where we discussed the properties of the diffusion tensor only in certain limits relevant to particular experimental situations. Here we shall systematically consider the temperature and coverage dependence of the diffusion tensor in the model. We have generalized our original model[14] to consider the role of intrinsic prefactors of the jump rates in determining the effective prefactors of the diffusion coefficients. Also a more detailed description of the analytic and numerical work involved is given.

The organization of the present work is as follows. In Sec. II we present the model we use to describe diffusion on a stepped substrate. The different theoretical approaches to solve the model are discussed in Sec. III. In Sec. IV we present the results for the components of the collective diffusion tensor in various limits. We also apply our results to analyze recent surface diffusion data obtained for the system CO/Ni(110).[5,6] Section V comprises a discussion of the main implications of our results.

II. MODEL AND ITS STATIC PROPERTIES

Following the earlier work dealing with the zero-coverage limit,[9] we introduce several energy barriers in our model characterizing the adsorption on the stepped substrate. The corresponding potential profile in direction perpendicular to step edges (x direction) is shown in Fig. 1(a). An additional

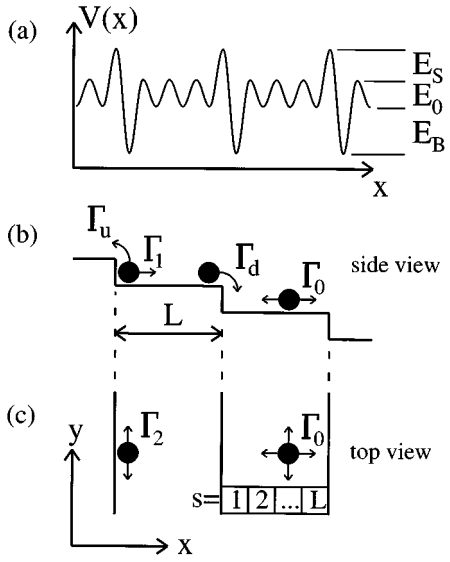

FIG. 1. Geometry and jump rates of the lattice model for diffusion on a stepped substrate. (a) The potential profile in x direction. (b) Side view of the model showing the various intrinsic hopping rates for jumps in x direction near step edges. The rate Γ_1' (not shown) is the rate for the process reverse to that with the rate Γ_1. (c) Top view of the model showing the size of one unit cell with the indices $s=1,2,\ldots,L$ of each lattice site within the cell.

binding energy E_B at the lower step edges can arise as a consequence of extra coordination for the adsorption sites there. Similarly, a Schwoebel barrier E_S for jumps from the terrace to the lower step edges[3] can exist due to the reduced coordination at the saddle point compared to the one for a jump on a terrace, for which the activation barrier is denoted by E_0. In this work, the barrier for jumps along lower step edges, E_2, is taken to be lower than E_0, leading to a higher jump rate along the lower step edges. The inert substrate surface is assumed to have a periodic array of straight steps separated by terraces of width of L lattice sites.

The energy barriers lead to the following rates for nearest-neighbor jumps as shown in Fig. 1(b) and Fig. 1(c): Γ_0 on the terraces, Γ_1 from the lower edge to the same terrace, Γ_1' from the terrace to lower edge, Γ_u from the lower edge across the step up to the neighboring terrace, Γ_d from the upper edge across the step down to the lower edge on the neighboring terrace, and Γ_2 along the lower step edge. We have generalized the set of rates used in Refs. 9 and 14 by allowing for modified prefactors ν_S, ν_B and ν_2, for jumps over step edge, detachment from (attachment to) step edge, and jumps along the lower step edge, respectively. The generalized set of rates can now be written as

$$\Gamma_0=\nu_0 e^{-E_0/kT}=\frac{\nu_0}{\nu_B}\xi\Gamma_1=\frac{\nu_0}{\nu_B}\Gamma_1'=\frac{\nu_0}{\nu_S}\sigma\Gamma_d=\frac{\nu_0}{\nu_S}\xi\sigma\Gamma_u, \tag{2.1}$$

$$\Gamma_2=\nu_2 e^{-E_2/kT}, \tag{2.2}$$

where the parameters ξ and σ defined by $\xi=e^{E_B/kT}$ and $\sigma=e^{E_S/kT}$ describe the effective strengths of the binding at step edge and the Schwoebel barrier. Each adsorption site is labeled by the coordinate (lLa,mb) of the unit cell together with a site index $s=1,2,\ldots,L$ within the unit cell [see Fig. 1(c)]. Here a and b are the nearest-neighbor distances along the x and y directions, respectively. For each site we then define a stochastic occupation variable $n_{l,m}^s(t)$, which due to the exclusion of double occupancy can take on only the values 0 and 1.

In the present model, the adsorption potential is modified only for lattice sites at the lower step edge, and therefore we have only two distinct row coverages c_e and c_t, for lower step edges and terraces, respectively, defined by

$$c_e=\langle n_{l,m}^1\rangle, \quad c_t=\langle n_{l,m}^2\rangle=\langle n_{l,m}^3\rangle=\cdots=\langle n_{l,m}^L\rangle. \tag{2.3}$$

These occupation numbers are independent of the cell indices (l,m) by symmetry, and they obey the detailed balance condition[15]

$$\frac{c_e(1-c_t)}{c_t(1-c_e)}=\xi, \tag{2.4}$$

which allows us to express c_e and c_t as a function of the total coverage $c=c_t+(c_e-c_t)/L$ as

$$c_e=c_e(\xi,L,c)=\frac{1}{2(\xi-1)}(\beta_+-\sqrt{\beta_-^2+\alpha}),$$
$$c_t=c_t(\xi,L,c)=\frac{1}{2(\xi-1)(L-1)}(\beta_-+\sqrt{\beta_-^2+\alpha}), \tag{2.5}$$

where $\beta_\pm=(\xi-1)(Lc\pm1)\pm L$ and $\alpha=4(\xi-1)(L-1)Lc$.

Under conditions typical to experiments on smooth surfaces, the value of the terrace width L ranges from 50 to 500, and the extra binding at the step edges, characterized by $\xi=e^{E_B/kT}$, satisfies the condition $\xi\gg1$. Equation (2.5) then leads to the following observations. At very low coverages such that $c\leqslant 1/L$, the particles adsorb preferentially at the step edges because of the extra binding there so that $c_e\approx cL$ while terraces are practically empty with $c_t\approx 0$.[16] This situation continues as the coverage is increased until one reaches the value $c=1/L$. At this point, the step edges are fully occupied and the terraces remain empty with $c_e\approx 1$ and $c_t\approx 0$. Beyond that point, for $c>1/L$, terraces start to be populated while the edge rows remain fully occupied, i.e. $c_e\approx 1$ with $c_t\approx c$. This can be seen more explicitly by expanding c_e and c_t in Eq. (2.5) to lowest order in the deviation $c-1/L$. For $\xi\gg L$ we find

$$c_e\approx 1-\sqrt{\frac{L-1}{\xi}}+\frac{L}{2}\left(c-\frac{1}{L}\right)+O\left(\left(c-\frac{1}{L}\right)^2\right),$$
$$c_t\approx \sqrt{\frac{1}{(L-1)\xi}}+\frac{L}{2(L-1)}\left(c-\frac{1}{L}\right)+O\left(\left(c-\frac{1}{L}\right)^2\right). \tag{2.6}$$

This behavior of c_e and c_t is the key to understand the variation of the diffusion constant with the coverage c. Since typically for large terrace width $1/L\leqslant$ few percent, the experimental situation usually corresponds to the regime $c>1/L$, and the influence of the steps on the measured values of diffusion rates differs substantially from the zero-coverage behavior described in Ref. 9.

As will be shown in the next section, a large part of the coverage dependence of the collective diffusion comes from the so-called ''*thermodynamic factor*'' f defined as[4]

$$f=\frac{\langle N_A\rangle}{\langle (N_A-\langle N_A\rangle)^2\rangle}\equiv\frac{c}{T}\frac{\partial\mu}{\partial c}, \tag{2.7}$$

which is inversely proportional to the compressibility of the adsorbate layer. In the Langmuir gas model, f can be evaluated exactly and is given by

$$f=\frac{Lc}{(L-1)(1-c_t)c_t+(1-c_e)c_e}. \tag{2.8}$$

When the coverage first increases from the initial zero value, the adparticles are preferentially adsorbed at the edge rows due to the extra binding there. The suppression of the fluctuations in the occupation of the edge rows then leads to an initial increase of f with the coverage. At $c=1/L$, the edge rows are completely occupied and the terraces are empty. This results in maximum suppression of the occupancy fluctuations, leading to a maximum in f. On further increase of the coverage, the edge rows remain fully occupied but the terraces become partially occupied and hence the compress-

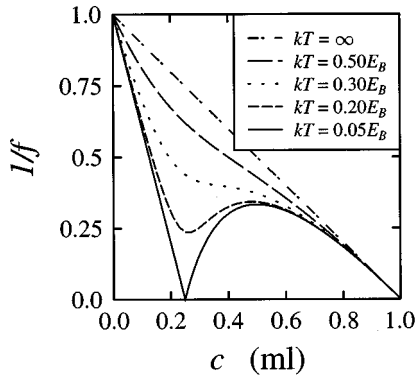

FIG. 2. Inverse of the thermodynamical factor f as given by Eq. (2.8) at different temperatures as a function of coverage for $L=4$.

ibility increases and f decreases. The behavior of f for $L=4$ for several temperatures kT/E_B is shown in Fig. 2, from which we see that f decreases very rapidly with decreasing temperature at $c=1/L$. The behavior of f near $c=1/L$ for $e^{E_B/kT} \gg L$ can be obtained by substituting Eq. (2.6) into Eq. (2.8), leading to the expression

$$f \approx \frac{e^{E_B/2kT}}{2\sqrt{L-1}}, \tag{2.9}$$

which with decreasing temperature results in an exponentially increasing thermodynamical contribution to the diffusion constant.

III. ANALYTICAL AND COMPUTATIONAL METHODS

The collective (chemical) diffusion tensor D can be conveniently defined through the decay of spontaneous density fluctuations. The density-fluctuation autocorrelation function $S(\mathbf{r},\mathbf{r}',t)$ is defined as

$$S(\mathbf{r},\mathbf{r}',t)=\sum_{s,s'} \langle [n^s_{l,m}(t)-\langle n^s_{l,m}\rangle][n^{s'}_{l',m'}(0)-\langle n^{s'}_{l',m'}\rangle]\rangle, \tag{3.1}$$

where the position vector of a unit cell is $\mathbf{r}=(lLa,mb)$, and the angle brackets denote an ensemble average. In the hydrodynamic limit $t\to\infty$ and $\mathbf{k}\to 0$, its Fourier transform with respect to unit cell indices behaves as $S(\mathbf{k},t) \sim \exp(-\mathbf{k}\cdot D\cdot \mathbf{k}t)$. Correspondingly, the Laplace transform $S(\mathbf{k},z)$ has a pole at $z=\mathbf{k}\cdot D\cdot \mathbf{k}$. Another approach for evaluation of the collective diffusion is via the Green-Kubo relation[4]

$$D_{\nu\nu}=f\lim_{t\to\infty}\frac{1}{4Nt}\left\langle \left[\sum_{i=1}^{N}[r^{(i)}_{\nu}(t)-r^{(i)}_{\nu}(0)]\right]^2\right\rangle, \tag{3.2}$$

where $r^{(i)}_{\nu}$ refers to the component $\nu=x,y$ of the position of adparticle i, the sum is over all particles, and f is exactly the thermodynamic factor introduced in Eq. (2.7) of the preceding section.

We have used two equivalent analytic approaches to calculate collective diffusion: the Mori projection operator formalism[10] and the Green's functions techniques.[11,12] In both approaches, the diffusion constant is obtained by identifying the pole of the density correlation function in the hydrodynamic limit as discussed above. The starting point is the rate equations for the stochastic occupancy variables $n^s_{l,m}(t)$. With the definitions of the various rates in the preceding section, these can be written as

$$\begin{aligned}
\frac{d}{dt}n^1_{l,m} &= -(\Gamma_1+\Gamma_u+2\Gamma_2)n^1_{l,m}+\Gamma_1' n^2_{l,m}+\Gamma_d n^L_{l-1,m} \\
&\quad +(\Gamma_1-\Gamma_1')n^2_{l,m}n^1_{l,m}+(\Gamma_u-\Gamma_d)n^L_{l-1,m}n^1_{l,m} \\
&\quad +\Gamma_2(n^1_{l,m+1}+n^1_{l,m-1}), \\
\frac{d}{dt}n^2_{l,m} &= -(3\Gamma_0+\Gamma_1')n^2_{l,m}+\Gamma_0 n^3_{l,m}+\Gamma_1 n^1_{l,m} \\
&\quad +(\Gamma_1'-\Gamma_1)n^1_{l,m}n^2_{l,m}+\Gamma_0(n^2_{l,m+1}+n^2_{l,m-1}), \\
\frac{d}{dt}n^s_{l,m} &= -4\Gamma_0 n^s_{l,m}+\Gamma_0 n^{s+1}_{l,m}+\Gamma_0 n^{s-1}_{l,m} \\
&\quad +\Gamma_0(n^s_{l,m+1}+n^s_{l,m-1}) \quad \text{for } 2<s<L, \\
\frac{d}{dt}n^L_{l,m} &= -(3\Gamma_0+\Gamma_d)n^L_{l,m}+\Gamma_u n^1_{l+1,m}+\Gamma_0 n^{L-1}_{l,m} \\
&\quad +(\Gamma_d-\Gamma_u)n^1_{l+1,m}n^L_{l,m}+\Gamma_0(n^L_{l,m+1}+n^L_{l,m-1}).
\end{aligned} \tag{3.3}$$

Next we generalize the standard description[17,18] of collective diffusion within the framework of the Mori formalism[10] to the case with substrate steps. The relevant dynamical variables are now the components

$$A^s_0(\mathbf{k},t)=\sum_{l,m}[n^s_{l,m}(t)-\langle n^s_{l,m}\rangle]\exp[i(lLak_x+mbk_y)] \tag{3.4}$$

of the L-dimensional vector $\mathbf{A_0}=(A^1_0,A^2_0,\ldots,A^L_0)$. The quantity of interest is the Laplace transform of the $L\times L$ density-fluctuation correlation matrix

$$\mathbf{Y}(\mathbf{k},z)=\int_0^\infty e^{-zt}\langle \mathbf{A_0}(\mathbf{k},t)|\mathbf{A_0}(\mathbf{k})\rangle dt, \tag{3.5}$$

where the angle brackets denote thermodynamical averages and $\mathbf{A}_0(\mathbf{k})\equiv\mathbf{A}_0(\mathbf{k},0)$. Using the projection operator techniques it can be formally expressed as

$$\mathbf{Y}(\mathbf{k},z)=\frac{\chi(\mathbf{k})}{z\mathbf{1}+\mathbf{b}(\mathbf{k})\chi(\mathbf{k})^{-1}+\mathbf{M}_1(\mathbf{k},z)}, \tag{3.6}$$

where the ''jump rate matrix'' $\mathbf{b}(\mathbf{k})=-\langle \mathbf{A_0}(\mathbf{k})|d/dt\mathbf{A_0}(\mathbf{k})\rangle$ and the ''susceptibility matrix'' $\chi(\mathbf{k})=\langle \mathbf{A}_0(\mathbf{k})|\mathbf{A}_0(\mathbf{k})\rangle$. The memory function $\mathbf{M}_1(\mathbf{k},z)$ originates from the the correlation effects between successive individual adparticle jumps. To proceed further, we will set $\mathbf{M}_1(\mathbf{k},z)$ to zero. This corresponds to a dynamical mean-field (DMF) approximation. For the Langmuir gas model in the absence of steps, the correlation effects cancel out exactly for collective diffusion,[19] and DMF is exact. For the stepped surface, we will show below by comparison with direct Monte Carlo simulation studies that DMF remains a very good approximation.

As discussed earlier, the diffusion tensor D can be extracted from the poles of $S(\mathbf{k},z)\equiv\Sigma_{s,s'}\mathbf{Y}_{s,s'}(\mathbf{k},z)$. According to Eq. (3.6) with $\mathbf{M}_1(\mathbf{k},z)=0$, each of the elements $\mathbf{Y}_{s,s'}(\mathbf{k},z)$ is inversely proportional to $\det[z\mathbf{1}+\mathbf{b}(\mathbf{k})\chi(\mathbf{k})^{-1}]$ and, therefore, the diffusive pole of $S(\mathbf{k},z)$ at $z=\mathbf{k}\cdot D\cdot\mathbf{k}$ can be determined from the zeros of this determinant in the limit $\mathbf{k}\to 0$ and $\omega\to 0$. By expanding the determinant (see the Appendix), collecting the leading terms for small ω and $\mathbf{k}$, we find the diagonal elements of D to be

$$D_{xx}=\frac{f}{Lc}\,\frac{(1-c_e)(1-c_t)c_t\Gamma_0L^2a^2}{(L-2)(1-c_e)+(1-c_t)[\nu_0/\nu_B+(\nu_0/\nu_S)\sigma]},$$

$$D_{yy}=\frac{f}{Lc}[(L-1)(1-c_t)c_t\Gamma_0+(1-c_e)c_e\Gamma_2]b^2. \tag{3.7}$$

Here f is the thermodynamic factor given by Eq. (2.8), so the result for D in Eq. (3.7) is indeed of the form given by the Green-Kubo formula Eq. (3.2). Combining Eqs. (3.7) and (2.8) and using the detailed balance condition of Eq. (2.4) leads to the form

$$D_{xx}=\frac{\Gamma_0L^2a^2}{[L-1+(c_e/c_t)^2\xi^{-1}][L-2+(c_t/c_e)[\nu_0/\nu_B+(\nu_0/\nu_S)\sigma]\xi]}, \tag{3.8}$$

$$D_{yy}=\left\{1+\frac{(\Gamma_2/\Gamma_0-1)}{1+(L-1)(c_t/c_e)^2\xi}\right\}\Gamma_0b^2, \tag{3.9}$$

which will be useful in our discussion of the coverage dependence of D. By symmetry, the nondiagonal elements of D are identically zero.

It is easy to see that the DMF results of Eqs. (3.8) and (3.9) are exact in the following cases. First, for $E_B=0$ we have $c_e=c_t=c$ with $\Gamma_1=\Gamma_1'$ and $\Gamma_u=\Gamma_d$ so that all the higher-order terms, i.e., the products of two occupation variables, in Eq. (3.3) cancel out, and the final result is independent of coverage.[19] The other special cases are $c\to 0$ and $c\to 1$. These limits correspond to diffusion of a single adparticle or a single vacancy and therefore the correlation effects vanish and DMF is exact.

In our previous treatment of this problem[14] we formulated the theory in terms of the Green's functions method,[11,12] where the coupled equations of motion for the Green's functions

$$G^{ss'}_{lml'm'}(t)\equiv-2\pi i\,\theta(t)\langle[n^s_{lm}(t)-c_s][(n^{s'}_{l'm'}(0)-c_{s'}]\rangle \tag{3.10}$$

can be solved by decoupling the higher-order Green's functions

$$G^{ss's''}_{lml'm'l''m''}(t)=-2\pi i\,\theta(t)\langle[n^s_{l,m}(t)-c_s][n^{s'}_{l',m'}(t)-c_{s'}]\times[n^{s''}_{l'',m''}(0)-c_{s''}]\rangle, \tag{3.11}$$

where $\theta(t)$ is the Heaviside step function. After Fourier transforming the resulting mean-field equations with respect to time and unit cell coordinates, a closed set of equations for $G^{ss'}_{\mathbf{k}}(\omega)$ is obtained. The study of diffusive poles then leads to the evaluation of the same determinant and to the same final result for D as obtained above using the projection operator techniques. In this paper we shall not discuss the Green's functions formalism in more detail; major differences between these two formalisms appear only in the way possible higher-order approximations are constructed.[10–12]

To test our analytical results, we have performed MC simulations[13] using both the density-fluctuation and the Green-Kubo methods to compute D. A detailed discussion and a comparison of these methods as tools in numerical work can be found in Ref. 20 and an application to a case of

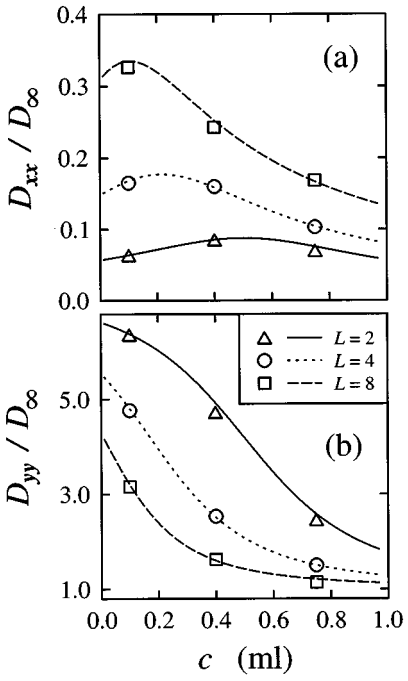

FIG. 3. Analytic and Monte Carlo results for D_{xx} and D_{yy} as a function of coverage for $E_B/kT=E_S/kT=(E_0-E_2)/kT=2$ with $\nu_0=\nu_S=\nu_B$. Lines show the dynamical mean-field theory of Eq. (3.7), and plotting symbols denote the results of Monte Carlo simulations with error bars less than the size of the symbols. Here diffusion coefficients are shown in units of $D_\infty=\Gamma_0a^2$, that is, the value for infinite terrace width and coverage in units of one monolayer so that the value of E_0 does not need to be specified.

a stepped substrate in Ref. 8. The coverage dependence of D as given by Eq. (3.7) together with the MC simulation results using the Green-Kubo method are shown in Fig. 3 for a temperature comparable to the various activation barriers in the system, $E_B/kT=E_S/kT=(E_0-E_2)/kT=2$, and with identical intrinsic prefactors $\nu_0=\nu_S=\nu_B$. With this choice, the ratio of the fastest and slowest jump rate is approximately 400, and going further down in temperature would increase the computational cost considerably. To compute the diffusion constant, we have to study the $\mathbf{k}\to 0$ limit. The smallest value of k_x is equal to $2\pi/N_x$, where N_x is the number of unit cells each containing L sites. The accurate determination of the diffusion constant therefore requires a large system size. Typical simulation parameters to produce Fig. 3 were 10^8 MC steps per atom for about 1000 atoms. The size of the simulation cell, depending on coverage and the terrace width $2\leqslant L\leqslant 8$, varied up to $\max(N_x)=64$ and $\max(N_y)=128$. Long simulation time was needed to reveal the fine structure in the coverage dependence of D_{xx}. We have performed a similar set of simulations for $E_B/kT=E_S/kT=(E_0-E_2)/kT=1/2$, where simulations are easier, but the coverage dependence of D is much weaker. The results plotted in Fig. 3 show that between its exact limits $c\to 0$ and $c\to 1$ the analytic theory agrees very well with the MC data, with no discernible systematic deviation. Thus the DMF provides a very accurate description of the present system.

In the remainder of this paper we shall use the analytic DMF result as given by Eqs. (3.8) and (3.9) to study the properties of D in various limits. For the reasons explained above, computational effort in the MC simulations increases rapidly for increasing terrace width, and a full numerical study of stepped surfaces with realistic terrace widths and system sizes is not feasible. The analytic DMF developed here thus provides an accurate and powerful tool for studying problems such as the crossover from step-dominated to terrace-dominated diffusion as a function of temperature and terrace width.

IV. PROPERTIES OF THE DIFFUSION TENSOR

In this section we shall consider the coverage and temperature dependence of the diffusion tensor D as given by Eqs. (3.8) and (3.9). As explained above, for $E_B=0$ all row coverages are equal with $c_e\equiv c_t\equiv c$ so that all coverage dependence of D cancels out, and even with large Schwoebel effect the properties of D are relatively simple. Therefore the main emphasis will be on cases where the extra binding at step edge is strong, i.e., $\xi=e^{E_B/kT}\gg 1$.[21] Based on the analysis below, behavior of D in other cases can be easily understood.

A. Diffusion perpendicular to step edges

At low coverages such that $c<1/L$, behavior of D_{xx} can be understood by examining the zero-coverage limit of Eq. (3.8). In this limit $c_e/c_t=e^{E_B/kT}$ so that Eq. (3.8) reduces to

$$D_{xx}^{c\to 0}=\frac{\Gamma_0 L^2 a^2}{[L-1+e^{E_B/kT}][L-2+\nu_0/\nu_B+(\nu_0/\nu_S)e^{E_S/kT}]}, \tag{4.1}$$

in agreement with the result of Ref. 9. In Eq. (4.1), the effect of the extra binding energy E_B and that of the Schwoebel barrier E_S appear in different factors of the denominator. Note that the first factor containing the effect of E_B comes from the $c\to 0$ limit of the thermodynamic factor f, which is a static property and, therefore, is not affected by the intrinsic prefactors.[15] Evidently, for $e^{E_B/kT}\gg 1$, the L dependence of Eq. (4.1) is very different in cases $e^{E_S/kT}\gg L$ and $e^{E_S/kT}\ll L$.

As the coverage increases, the value of D_{xx} increases with increasing coverage and reaches a maximum at $c=1/L$ before starting to decrease as c increases further. This behavior is illustrated in Fig. 3(a). This somewhat surprising result can be understood from the Green-Kubo relation in Eq. (3.2). Obviously, the center-of-mass mobility cannot have any special behavior at the point $c=1/L$, so that this special coverage variation of D_{xx} comes entirely from the coverage dependence of the thermodynamic factor f as detailed earlier by Eq. (2.9) and Fig. 2. Note that for decreasing temperature f increases exponentially and can therefore partially compensate the effect of the decreasing intrinsic jump rates at step edges.

Since step spacings of the order of a few hundred lattice constants can be achieved for good sample surfaces, the regime $c\gg 1/L$ is the most relevant one for most experiments. In this limit, with $e^{E_B/kT}\gg 1$ and $L\gg 1$, we have $c_e\approx 1$ and $c_t\approx c$, and the expression of D_{xx} in Eq. (3.8) reduces to

$$D_{xx}\approx\frac{\Gamma_0 L a^2}{L+c[\nu_0/\nu_B+(\nu_0/\nu_S)e^{E_S/kT}]e^{E_B/kT}}. \tag{4.2}$$

With fixed values of intrinsic barriers and prefactors, this expression is an increasing function of L and a decreasing function of c. The $1/c$ behavior of D_{xx} at large c is visible already in the result for $L=8$ in Fig. 3(a).

B. Diffusion parallel to step edges

In general, diffusion in the direction parallel to the steps appears to have a relatively simple dependence on coverage and terrace width. The zero-coverage limit of D_{yy} is particularly simple: In the absence of blocking we have $c_e/c_t\approx=e^{E_B/kT}$ so that Eq. (3.9) leads to

$$D_{yy}^{c\to 0}=\left(1+\frac{\Gamma_2/\Gamma_0-1}{1+(L-1)e^{-E_B/kT}}\right)\Gamma_0 b^2, \tag{4.3}$$

which is the result obtained in Ref. 9. Here the effects of the extra binding and the enhanced jump rate at step edges *both* increase D_{yy}.

In the case of D_{yy}, the minimum in the compressibility close to $c=1/L$ due to the suppression of the fluctuations (cf. Sec. IV A) is largely canceled out by the enhanced blocking of jumps along the lower step edges when $c_e\approx 1$. This leads to the monotonically decreasing behavior of D_{yy} as a function of coverage at low coverages as shown in Fig. 3(b). There is no peak at the special value of $c=1/L$ as shown in the case of D_{xx}.

For a fixed coverage $c\gg 1/L$ at low temperature two effects compete with each other. First, for $E_2<E_0$ the ratio $\Gamma_2/\Gamma_0\propto e^{(E_0-E_2)/kT}$ and diffusion along the step edge row is increasingly faster than in the terrace region. At the same

time, the occupation of the edge row increases as the factor $\xi = e^{E_B/kT}$, which leads to an exponential increase in the blocking factor for diffusion along the step edge. These two effects determine the coverage and temperature dependence of the diffusion in the direction parallel to the steps. In the low temperature limit with $L \gg 1$, we have $c_e \approx 1$ and $c_t \approx c$ so that Eq. (3.9) reduces to

$$D_{yy} \approx \left(1 + e^{(E_0 - E_2 - E_B)/kT} \frac{\nu_2}{L \nu_0 c^2} \right) \Gamma_0 b^2. \tag{4.4}$$

From this form we see that for $E_0 - E_2 > E_B$ the main contribution at low temperature comes from diffusion along the lower step edge, i.e., from the second term on the right-hand side. If, on the other hand, $E_0 - E_2 < E_B$, then at low temperature the increase in the edge rate Γ_2 is not big enough to compensate the enhanced blocking, and the less-blocked terrace jumps with rate Γ_0 dominate. In other words, D_{yy} depends on whether the larger proportion of mass transport occurs at step edges or on terraces.

C. Crossover from step-dominated to terrace-dominated diffusion

At high temperature or for very wide terraces, diffusion *perpendicular* to the steps is expected to be dominated by the terrace rate Γ_0, and the effect of the steps vanishes. In the other limit of low temperature and narrow terraces, the slower jump rates at step edges become the rate-limiting factor. Next we examine the *crossover* from the step-dominated to terrace-dominated regime.

In the low-coverage limit $c \ll 1/L$, we see immediately from Eq. (4.1) that the crossover occurs at $L \approx \max(e^{E_B/kT}, \nu_0/\nu_B + (\nu_0/\nu_S) e^{E_S/kT})$. For terrace widths much larger than this crossover value, the effect of the steps is negligible, whereas for terrace widths much smaller than this value, the step barriers and prefactors dominate the diffusion constant. In the experimentally more relevant high-coverage limit $c \gg 1/L$, the crossover criterion is quite different from the low-coverage situation. According to Eq. (4.2), it is now determined by the condition

$$L \approx c \left(\frac{\nu_0}{\nu_B} + \frac{\nu_0}{\nu_S} e^{E_S/kT} \right) e^{E_B/kT}. \tag{4.5}$$

For L much smaller than this crossover value, the diffusion constant D_{xx} is again dominated by the steps and the barriers at the step edges. We note that in the step-dominated regime, in general the diffusion constant has a complicated temperature dependence and not the simple Arrhenius form. The exact temperature dependence can be obtained explicitly from Eq. (3.8) and depends on a complicated interplay of the intrinsic activation barriers, prefactors, and the terrace width.

Instead of considering all the possible variations, we illustrate the crossover behavior for one particular case, namely, the case $e^{E_B/kT} \gg 1$ with $c \gg 1/L$ and $L \gg 1$ described by Eq. (4.2) above. We shall take $e^{E_S/kT} \approx 1$, which corresponds to a negligible Schwoebel effect within the temperature range of interest. Other cases as well as the crossover at lower coverages can be treated in an analogous way using the expressions for D_{xx} given in Sec. IV A. With the given conditions, we observe immediately from Eq. (4.2) that the effect of the binding energy E_B is comparable to that of the terrace barrier E_0 within a crossover regime characterized by

$$L \approx c \left(\frac{\nu_0}{\nu_B} + \frac{\nu_0}{\nu_S} \right) e^{E_B/kT}. \tag{4.6}$$

For this regime, the temperature dependence of D_{xx} cannot be described by the simple Arrhenius form. In the terrace-dominated regime, i.e., for $L \gg c(\nu_0/\nu_B + \nu_0/\nu_S) e^{E_B/kT}$, we obtain from Eq. (4.2) the expected form

$$D_{xx} \approx \nu_0 a^2 e^{-E_0/kT}, \tag{4.7}$$

where diffusion is characterized by the terrace energy barrier E_0 and the terrace prefactor ν_0. In the the step-dominated regime, i.e., for $L \gg c(\nu_0/\nu_B + \nu_0/\nu_S) e^{E_B/kT}$, we get

$$D_{xx} \approx \frac{La^2}{c(\nu_B^{-1} + \nu_S^{-1})} e^{(E_0 + E_B)/kT}. \tag{4.8}$$

Clearly Eq. (4.8) is of the Arrhenius form

$$D_{xx} = \nu_{\text{eff}} a^2 e^{-E_{\text{eff}}/kT}, \tag{4.9}$$

with an energy barrier $E_{\text{eff}} = E_0 + E_B$. Another important observation is that the *effective* prefactor $\nu_{\text{eff}} = L/c(\nu_B^{-1} + \nu_S^{-1})$ of the exponential form contains an additional factor L.[22]

Next we show how this theory can be used to analyze the effect of steps in a typical experimental situation. As an example, we shall discuss the recent measurements of diffusion of CO on Ni(110) surface through the optical grating method.[5–7] We concentrate on the data for diffusion along the $(1\,\bar{1}\,0)$ direction at the coverage 0.98. We expect our model to describe this case rather well, especially for the high-coverage limit $c \to 1$, which can be interpreted as diffusion of an isolated *vacancy* in the adlayer. Then the effect of possible adsorbate interactions is mainly to renormalize the microscopic activation barriers and intrinsic prefactors of the local jump rates of the vacancy on terraces and at step edges. Also, for large molecules like CO the simple blocking picture of our model is supposedly valid for processes at step edges. Note that for small (compared to step height) adsorbates this is not necessarily always true because particles hopping from the upper terrace over the step edge could then jump on top of the adsorbate layer on the lower terrace, i.e., into the second layer. Since the influence of steps is expected to be dominantly due to diffusion across step edges,[5–7] we shall below use our results for D_{xx}.

From a measurement on a good sample with $L \approx 520$, Xiao and co-workers obtained an activation barrier of 95 meV.[6,7] Based on another measurement for a sample with a higher step density they estimate the value of the step-dominated barrier to be $E_{\text{eff}} = 239$ meV.[23] Then they use a crossover criterion obtained by heuristic arguments,[5] which can be written in our notation as $L^2 \approx e^{(E_{\text{eff}} - E_0)/kT}$ for the case of equal prefactors for all jumps. Based on this form, these authors concluded that in the experimental temperature range of 100–200 K with $L \approx 520$ the effect of steps should be negligible and the value of 95 meV should represent the diffusion barrier along the $(1\,\bar{1}\,0)$ direction for the clean surface. The crossover criterion we obtained analytically,

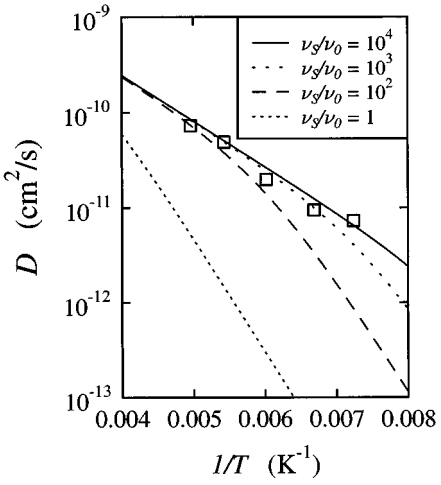

FIG. 4. Arrhenius plots of D_{xx} using experimental estimates for activation barriers for diffusion of CO on Ni(110) (Refs. 6, 7, and 23). Our theory for different choices of the ratio ν_S/ν_0 of the intrinsic prefactors is shown by lines. Note that the value of ν_0 only shifts the curves in vertical direction; we have chosen the value $\nu_0 = 2\times 10^{-8}$cm^2/s to obtain a good fit for large values of ν_S/ν_0. The experimental data points from Ref. 6 are denoted by squares. See text for detailed parametrization.

namely, Eq. (4.6), is quite different, with L instead of L^2 on the left-hand side. Next we examine using our analysis whether the effect of steps in this case can indeed be negligible.

As explained above, for coverage close to one, the various activation barriers in the system can be interpreted as barriers experienced by a single vacancy. Then, following Ref. 5, we can in our theory set $E_0 = 95$ meV and $E_0 + E_B + E_S = 239$ meV, which values through the experimental measurement also include the effect of adparticle interactions. To proceed further, we observe that with $E_S = 0$ (Ref. 24) in Eq. (4.2), we can without a loss of generality take $\nu_S = \nu_B$. With these choices and $c = 0.98$, the only free parameters left in Eq. (4.2) are ν_0 and the ratio ν_S/ν_0. In Fig. 4, we show the Arrhenius plot of D vs $1/T$ as given by our theory for different values of the prefactor ratio ν_S/ν_0. First consider the curve for equal prefactors with $\nu_S/\nu_0 = 1$. Clearly in the experimental temperature range, the step effects are not negligible and the effective barrier observed is considerably higher than the input value 95 meV, actually very close to the step-dominated value 239 meV, as expected on the basis of the crossover criterion of Eq. (4.6). Two possibilities remain.[25] One is that the intrinsic barrier is substantially smaller than the quoted value of 95 meV. The other is that the prefactor ν_S at the step edges is considerably larger than the intrinsic prefactor ν_0 on the terraces so that this *compensation* effect reduces the influence of the steps on the measured value of the barrier. To test this hypothesis, we show in Fig. 4 also the ''best fits'' to the experimental data set from Ref. 6 for larger values of ν_S/ν_0. Clearly the fits with $\nu_S/\nu_0 = 10^3$ and 10^4 are within reasonable experimental error bars, and with increasing the ratio ν_S/ν_0 the theoretical curve gets more linear, i.e., further away from the step-dominated regime.

The possible difference of ν_S and ν_0 arises from the entropy factors for the jumps at step edges as well as the nonadiabatic frictional coupling to the substrate excitations at the step edges, which are substantially different from that on terraces. The effective prefactor $\nu_{\rm eff}$ measured on a high step density surface[23] is indeed several orders of magnitude larger than the corresponding value on a surface with low step density. Because the experiment probes the *effective* prefactor, at least part of the increase in the measured value in the prefactor is due to the extra factor of L in $\nu_{\rm eff}$, as demonstrated above by Eq. (4.8). Also, other parameters such as impurity concentrations may be different for the two samples.[23] Thus it remains an open question whether the *intrinsic* prefactors ν_S and ν_0 can differ by almost three orders of magnitude. This is an important and fundamental question that remains to be investigated.

V. DISCUSSION

To summarize, we have presented a theoretical analysis of collective diffusion on stepped substrates, and studied the dependence of the diffusion tensor on the terrace width, coverage, and temperature in the case where on-site blocking is the dominant interaction between the adsorbate particles. In particular, we have established criteria for crossover from terrace-dominated diffusion to step-dominated diffusion. Compared with the heuristic criterion used before,[5,7] our theory predicts a much stronger influence of the steps on the diffusion barrier. Our present results demonstrate that even for surfaces with low step densities under typical experimental conditions, the influence of steps on measured diffusion barriers *and* effective prefactors can still be considerable, and a careful theoretical analysis is needed to understand the detailed influence of the steps on the diffusive motion of the adsorbates.

The effect of the steps on collective diffusion at finite coverages turns out to be very different from the corresponding result in the zero-coverage limit. This is true especially for diffusion perpendicular to the steps, described by D_{xx}. Due to the compressibility contribution to D_{xx}, considerable deviations from the zero-coverage behavior appear already at coverages near $c = 1/L$. The compressibility has a strong minimum at this coverage due to the preferential filling of the step edge sites, leading to a corresponding maximum in D. This effect is not just peculiar to the Langmuir gas model studied here, but should persist in systems with direct adparticle interactions as well.[26] Experimental observations of this effect should be feasible for vicinal substrates with narrow terraces.

The generic form of the criterion for the crossover from step-dominated to terrace-dominated diffusion at high coverage can be written as $L \approx \Gamma_{\rm flat}/\Gamma_{\rm step}$, where $\Gamma_{\rm flat}$ characterizes diffusion within the flat terrace region and $\Gamma_{\rm step}$ describes diffusion across step edges.[27] Different chacraterizations of the barriers and prefactors near the steps would only lead to a different form of $\Gamma_{\rm step}$, but do not change qualitatively the dependence on terrace width presented here. This form should be valid even in the presence of short-range adsorbate interactions, as long as the local coverage and the microscopic jump rates are roughly constant through the terrace region so that rates are modified only in the immediate vicinity of step edges.[28] The values of the barriers and prefac-

tors of course would be modified by the interactions between the adsorbates.

For interacting adsorbates at submonolayer coverages, the possible complex behavior of compressibility at special points[29] can change the thermodynamical contribution to D. Also, in some cases for coverages considerably below one, a nonuniform coverage profile across the terrace region can be induced,[8,26,29] which naturally leads to a variation of the local jump rates there, and thereby to a more complex kinetic contribution to D. These effects can lead to a coverage dependence very different from that of the present model. We are now employing the DMF formalism in conjunction with numerical sampling of local jump rates to systematically explore the in teraction and impurity effects.[30,31]

ACKNOWLEDGMENTS

This work has been supported by the Academy of Finland (J.M.), Emil Aaltonen Foundation (J.M.), and by a grant from the Office of Naval Research (S.C.Y. and J.M.). Computational resources of the Theoretical Physics Computing Facility at Brown University are gratefully acknowledged.

APPENDIX

In this Appendix we shall outline the derivation of the elements of the diffusion tensor from the zeros of the determinant of the $L\times L$ matrix $\mathbf{V}=z\mathbf{1}+\mathbf{b}(\mathbf{k})\chi(\mathbf{k})^{-1}$ in the hydrodynamic limit $\mathbf{k}\rightarrow 0$ and $\omega\rightarrow 0$. The differentiation with respect to time in the jump rate matrix $\mathbf{b}(\mathbf{k})=\langle \mathbf{A_0}(\mathbf{k})|(d/dt)\mathbf{A_0}(\mathbf{k})\rangle$ can be carried out by substituting the rate equations of Eq. (3.3), after which the elements of $\mathbf{b}$ and also the elements of the susceptibility matrix $\chi(\mathbf{k})=\langle \mathbf{A_0}(\mathbf{k})|\mathbf{A_0}(\mathbf{k})\rangle$ are found using the following equal-time identity of the Langmuir gas model:

$$\langle (n^s_{lm}-c_s)n^{s'}_{l'm'}\rangle=\delta_{ss'}\delta_{ll'}\delta_{mm'}(1-c_s)c_s\,. \qquad \text{(A1)}$$

The resulting elements of $\mathbf{b}$ are combinations of average rates of occurrence of the different jumps of the form $\langle n^s_{lm}(1-n^{s'}_{l'm'})\Gamma_{s\rightarrow s'}\rangle=c_s(1-c_{s'})\Gamma_{s\rightarrow s'}$, where $(l,m;s)$ and $(l',m';s')$ refer to nearest-neighbor adsorption sites. After neglecting the memory function, the correlation matrix $\mathbf{Y}$ is inversely proportional to det$\mathbf{V}$, where the interior elements related to terrace jumps are given by

$$\mathbf{V}_{ss}=z-2\Gamma_0\cos k_y b+4\Gamma_0\,,$$

$$\mathbf{V}_{s,s\pm 1}=-\Gamma_0\,, \qquad \text{(A2)}$$

and the modified elements at the corners related to jumps near step edges are given by

$$\mathbf{V}_{11}=z-2\Gamma_2\cos k_y b+\Gamma_1+\Gamma_u+2\Gamma_2+(\Gamma_1'-\Gamma_1+\Gamma_d-\Gamma_u)c_t\,,$$

$$\mathbf{V}_{22}=z-2\Gamma_0\cos k_y b+3\Gamma_0+\Gamma_1'+(\Gamma_1-\Gamma_1')c_e\,,$$

$$\mathbf{V}_{LL}=z-2\Gamma_0\cos k_y b+3\Gamma_0+\Gamma_d+(\Gamma_u-\Gamma_d)c_e\,,$$

$$\mathbf{V}_{12}=-\Gamma_1-(\Gamma_1'-\Gamma_1)c_t\,,$$

$$\mathbf{V}_{21}=-\Gamma_1'-(\Gamma_1-\Gamma_1')c_e\,,$$

$$\mathbf{V}_{1L}=-[\Gamma_u+(\Gamma_d-\Gamma_u)c_t]e^{+iLk_x a},$$

$$\mathbf{V}_{L1}=-[\Gamma_d+(\Gamma_u-\Gamma_d)c_e]e^{-iLk_x a}. \qquad \text{(A3)}$$

The phase factors in Eqs. (A2) and (A3) arise from jumps from one unit cell to another, i.e., from all jumps in the y direction and from jumps across the step edges in the x direction. All the other elements of $\mathbf{V}$ are identically zero so that the matrix $\mathbf{V}$ is almost tridiagonal and det$\mathbf{V}$ can be evaluated after first expanding the minor involving only the middle elements of Eq. (A2) for general L. The element D_{xx}, e.g., is then extracted as the ratio a_x/a_z of the coefficients of the leading terms of $\det\mathbf{V}=za_z+a_xk_x^2+\cdots$ in the hydrodynamic limit $z\rightarrow 0$ and $k_x\rightarrow 0$ with $k_y=0$.

*Permanent address: Department of Physics, University of Jyväskylä, P.O. Box 35, FIN-40351 Jyväskylä, Finland.

[1] *Surface Mobilities on Solid Materials: Fundamental Concepts and Applications*, edited by V. T. Binh (Plenum Press, New York, 1981); *Kinetics of Ordering and Growth at Surfaces*, edited by M. G. Lagally (Plenum Press, New York, 1990).

[2] H. Wagner, in *Solid Surface Physics*, edited by G. Höhler (Springer, Berlin, 1979); J. Krug and H. Spohn, in *Solids far From Equilibrium*, edited by G. Godreche (Cambridge University Press, Cambridge, England, 1991).

[3] R. L. Schwoebel and E. J. Shipsey, J. Appl. Phys. **37**, 3682 (1966); G. Ehrlich and F. G. Hudda, J. Chem. Phys. **44**, 1039 (1966); R. L. Schwoebel, J. Appl. Phys. **40**, 614 (1969).

[4] R. Gomer, Rep. Prog. Phys. **53**, 917 (1990).

[5] X. D. Xiao, X. D. Zhu, W. Daum, and Y. R. Shen, Phys. Rev. B **46**, 9732 (1992).

[6] X. D. Xiao, Y. Xie, and Y. R. Shen, Phys. Rev. B **48**, 17 452 (1993).

[7] X. D. Xiao, Y. Xie, C. Jakobsen, H. Galloway, M. Salmeron, and Y. R. Shen, Phys. Rev. Lett. **74**, 3860 (1995).

[8] C. Uebing and R. Gomer, Surf. Sci. **306**, 419 (1994); **306**, 427 (1994); **317**, 165 (1994); C. Uebing, Phys. Rev. B **49**, 13 913 (1994).

[9] A. Natori and R. W. Godby, Phys. Rev. B **47**, 15 816 (1993).

[10] H. Mori, Prog. Theor. Phys. **33**, 423 (1965).

[11] R. A. Tahir-Kheli and R. J. Elliott, Phys. Rev. B **27**, 844 (1983); R. A. Tahir-Kheli, *ibid.* **27**, 6072 (1983); **37**, 6072 (1985).

[12] T. Ala-Nissila, J. Kjoll, S. C. Ying, and R. A. Tahir-Kheli, Phys. Rev. B **44**, 2122 (1991).

[13] K. Kehr, in *Applications of the Monte Carlo Method in Statistical Physics*, edited by K. Binder (Springer, Berlin, 1984).

[14] J. Merikoski and S. C. Ying, Surf. Sci. **381**, L623 (1997).

[15] To satisfy detailed balance corresponding to the potential profile of Fig. 1(a), the intrinsic prefactors were chosen to be symmetric with respect to reversal of each jump, i.e., the prefactors are identical for the rates Γ_d and Γ_u, and also for the pair Γ_1 and Γ_1'. Also the Schwoebel barrier results in a symmetric temperature-dependent modification of rates Γ_u and Γ_d by the factor σ. Therefore the prefactors ν_B and ν_S and the Schwoebel factor σ do not affect static quantities like c_e and c_t. Note that

these symmetry properties guarantee that there is no diffusion bias although the potential profile of Fig. 1(a) is asymmetric.

[16] At small coverage, only if L is very much larger than $\xi = e^{E_B/kT}$, the gain in entropy by spreading the adsorbates over the terrace can compete with the extra binding energy E_B at step edge even if $\xi \gg 1$.

[17] V. P. Zhdanov, Surf. Sci. **149**, L13 (1985); **257**, 63 (1991); **291**, 145 (1993).

[18] M. Torri, R. Ferrando, E. Scalas, and G. P. Brivio, Surf. Sci. **307-309**, 565 (1994).

[19] R. Kutner, Phys. Lett. **A81**, 239 (1981), and references therein.

[20] C. Uebing and R. Gomer, J. Chem. Phys. **95**, 7626 (1991); **95**, 7636 (1991); **95**, 7641 (1991); **95**, 7648 (1991); **100**, 7759 (1994); Surf. Sci. **331-333**, 930 (1995).

[21] Also, we assume implicitly in the discussion that $E_S \geqslant 0$ and $E_B \geqslant 0$. Our DMF results of Eqs. (3.8) and Eqs. (3.9) are naturally valid also for negative values of E_S or E_B, i.e., in the cases where some barriers at step edges are reduced from the terrace value E_0.

[22] It is easy to understand where this extra factor L comes from considering the single-particle limit with $E_B = 0$ and $E_S > 0$. For a single particle, we can use the general expression for tracer diffusion, $D = \Gamma \ell^2$, where Γ is a jump rate and ℓ is the jump length. Now at very low temperature, i.e., in the step-dominated regime, the time scales for terrace jumps and step crossings are very different, and what happens within the terrace can therefore be considered as an ''internal degree of freedom'' for each unit cell. Now the probability for the particle to be in a site from which it can jump to an adjacent unit cell in either direction is $1/L$ so that Γ is normalized by the factor $1/L$. On the other hand, the effective length for going from one unit cell to another is L so that the factor ℓ^2 gets normalized by L^2. These two effects multiplied amount to a factor of L. The cases with $E_B > 0$ can be explained in an analogous way, but the higher probability of finding the particle at step edge has to be taken into account. Similarly, in the case $c \to 1$, the appearance of the extra factor of L in ν_{eff} can be understood by considering the jumps of a single vacancy between adjacent unit cells.

[23] X. D. Xiao (private communication).

[24] For this system the Schwoebel barrier is believed to be very small; P. J. Feibelman (private communication).

[25] We have also checked that our conclusions do not change essentially if we allow a finite value for E_S. This is rather expected, because in the high-coverage limit the basic form of D_{xx} remains unchanged.

[26] J. Merikoski, J. Timonen, and K. Kaski, Phys. Rev. B **50**, 7925 (1994).

[27] The general L dependence of D in the limit $c \to 1$ is consistent with the well-known analog between diffusion in a system with several activation barriers and electric conductivity in a network of resistors. However, the effects of the thermodynamical factor and the site-dependent blocking at submonolayer coverage have no direct analog.

[28] On a more technical level, this means that step effects modify only the elements at the corners of the matrix $\mathbf{b}(\mathbf{k})$ containing the local jump rates as defined in Sec. III. This observation shows the usefulness of the decomposition into the kinetic and thermodynamic contributions inherent in Eq. (3.6).

[29] E. V. Albano, K. Binder, D. W. Heermann, and W. Paul, Z. Phys. B **77**, 445 (1989); Surf. Sci. **223**, 151 (1989); J. Chem. Phys. **91**, 3700 (1989).

[30] J. Merikoski and S. C. Ying (unpublished).

[31] For a general method for interacting systems see T. Hjelt, I. Vattulainen, J. Merikoski, T. Ala-Nissila, and S. C. Ying, Surf. Sci. **380**, L501 (1997).